Check for updates

RESEARCH ARTICLE

Silicon photomultipliers for enhanced lidar bathymetric applications

[version 1; peer review: awaiting peer review]

Khayala Huseynzada[1,2], Azer Sadigov[1,3,4], Svitlana Lyubchyk[4]

[1]İnstitute of Physics, Baku, Azerbaijan
[2]Mingachevir State University, Mingachevir, Azerbaijan
[3]Innovation and Digital Development Agency, Baku, Azerbaijan
[4]DeepTechLab, Lusófona University, Lisbon, Portugal

v1 **First published:** 12 Oct 2026, **6**:419
https://doi.org/10.12688/openreseurope.24505.1
Latest published: 12 Oct 2026, **6**:419
https://doi.org/10.12688/openreseurope.24505.1

Abstract

Background

Silicon photomultipliers (SiPMs) are emerging as promising photodetectors for bathymetric Light Detection and Ranging (LIDAR) because of their high photon detection efficiency (PDE), single-photon sensitivity, and low operating voltage. However, the limited fill factor of conventional surface-pixel SiPMs reduces their detection efficiency. This study evaluates the performance of a newly developed buried-pixel SiPM for bathymetric LIDAR applications.

Methods

The electrical and optical characteristics of the buried-pixel MAPD-3NM-II were experimentally investigated and compared with those of the commercial surface-pixel MPPC S12572-010P. Breakdown voltage, internal gain, and photon detection efficiency were measured using a pulsed single-photon counting technique with a 530 nm pulsed laser under identical overvoltage and equal-gain conditions.

Results

The MAPD-3NM-II exhibited a breakdown voltage of 52.3 V, compared with 68 V for the MPPC S12572-010P. At an overvoltage of 4 V, the MAPD-3NM-II achieved an internal gain of 1.2×10^5, whereas the MPPC reached 8.5×10^4. Under identical operating conditions, the MAPD-3NM-II demonstrated a photon detection efficiency of 32%, compared with 8% for the commercial detector. At equal internal gain,

Open Peer Review

Approval Status *AWAITING PEER REVIEW*

Any reports and responses or comments on the article can be found at the end of the article.

the MAPD-3NM-II maintained a PDE of 32%, while the MPPC reached 9.5%. The improved performance is attributed to the buried-pixel architecture with a 100% fill factor, which increases the effective photosensitive area and enhances photon collection.

Conclusions

The buried-pixel MAPD-3NM-II demonstrated superior photon detection efficiency and internal gain compared with the commercial surface-pixel MPPC S12572-010P. These results indicate that buried-pixel SiPM technology is a promising candidate for bathymetric LiDAR systems and other applications requiring highly sensitive photon detection.

Keywords
silicon photomultipliers (SiPM); bathymetric LIDAR, photon detection efficiency, underwater mapping

This article is included in the Horizon Europe gateway.

This article is included in the Marie-Sklodowska-Curie Actions (MSCA) gateway.

Corresponding author: Khayala Huseynzada (khayala.huseynzada@gmail.com)

Author roles: Huseynzada K: Visualization, Writing – Review & Editing; **Sadigov A**: Methodology, Project Administration, Resources, Writing – Original Draft Preparation, Writing – Review & Editing; **Lyubchyk S**: Data Curation, Project Administration

Competing interests: No competing interests were disclosed.

Grant information: This project has received funding from the European Union's Horizon Research and Innovation Programme under the Marie Sklodowska-Curie's AQUADETECT project (grant agreement ID 101298573) and the Azerbaijan Science Foundation, Grant No. AEF-MGC-2024-2(50)-16/04/1-M-04.
The funders had no role in study design, data collection and analysis, decision to publish, or preparation of the manuscript.

Copyright: © 2026 Huseynzada K *et al*. This is an open access article distributed under the terms of the Creative Commons Attribution License, which permits unrestricted use, distribution, and reproduction in any medium, provided the original work is properly cited.

How to cite this article: Huseynzada K, Sadigov A and Lyubchyk S. **Silicon photomultipliers for enhanced lidar bathymetric applications [version 1; peer review: awaiting peer review]** Open Research Europe 2026, **6**:419 https://doi.org/10.12688/openreseurope.24505.1

First published: 12 Oct 2026, **6**:419 https://doi.org/10.12688/openreseurope.24505.1

Introduction

Bathymetric LIDAR (Light Detection and Ranging) is a powerful remote sensing technology used for precise mapping of underwater topography. By emitting short laser pulses toward a water body and measuring the time delay of reflected signals from both the water surface and the seafloor, LIDAR systems enable high-resolution three-dimensional reconstruction of submerged terrain. This capability is essential for various applications, including coastal zone management, hydrographic surveying, environmental monitoring, and flood risk assessment.

Traditional bathymetric LIDAR systems predominantly rely on photomultiplier tubes (PMTs)[1,2] or avalanche photodiodes (APDs)[3] for photon detection. While effective, these detectors exhibit limitations in terms of size, operating voltage, mechanical sensitivity, and photon detection efficiency under turbid or low-illumination aquatic conditions. Moreover, increasing environmental demands for more compact, energy-efficient, and UAV-compatible LIDAR systems necessitate the adoption of alternative photodetector technologies.

Silicon Photomultipliers (SiPMs) have emerged as a compelling alternative due to their ability to operate in Geiger-mode, enabling single-photon sensitivity, high gain, and excellent timing resolution. Unlike traditional PMTs, SiPMs are solid-state devices,[4] offering advantages such as low bias voltage (20–70 V), immunity to magnetic fields, ruggedness, and potential for miniaturization and mass production. The high photon detection efficiency (PDE), particularly in the green and blue-green spectral bands optimal for water penetration (e.g., 515–550 nm), further strengthens their relevance for bathymetric LIDAR.[5]

Bathymetric LIDAR system

Bathymetric LIDAR (Light Detection and Ranging) is a laser-based remote sensing technology used to map underwater topography by measuring the time delay between the emission of laser pulses and the detection of their reflections from both the water surface and the seafloor. Mounted on aerial platforms such as drones, aircraft, or satellites, the system is designed to capture high-resolution, three-dimensional spatial data over shallow and coastal water bodies. The core principle of operation relies on the time-of-flight (ToF) method,[6] where the system calculates the distance traveled by light by measuring the interval between pulse emission and reception (Fig. 1).

Figure 1. Working principle of bathymetric LIDAR.

A typical bathymetric LIDAR system consists of a pulsed laser transmitter, an optical scanning unit (such as an oscillating mirror), a photodetector, and precise timing electronics, integrated with a positioning system that combines GNSS (Global Navigation Satellite System) and inertial measurement units (IMU). Among these components, the photodetector —most commonly implemented using silicon photomultiplier (SiPM) technology—plays a central role in determining the overall system performance. In particular, the photon detection efficiency (PDE) of the SiPM is one of the key parameters governing the signal-to-noise ratio, depth detection capability, and ultimately the spatial and depth resolution of the reconstructed bathymetric image. During operation, the system emits a laser pulse—most commonly in the green region of the visible spectrum (around 530 nm)—which is particularly suitable for water penetration due to its low absorption in clear water. Upon hitting the water surface, part of the pulse is reflected back and recorded as the first return, while the remaining energy penetrates the water column, reflects off the seafloor, and returns as the second signal. The difference in travel time between these two returns allows for the accurate determination of water depth using the relation $d = \frac{c*\Delta t}{2n}$,[7] where c is the speed of light in vacuum and n is the refractive index of water, approximately 1.33. The improvements in photodetector sensitivity—particularly through the use of high-PDE SiPMs—directly translate into enhanced timing precision, improved depth retrieval, and higher-quality bathymetric images.

Photodetector concepts and comparison

In the context of bathymetric LIDAR systems, the choice of photodetector architecture plays a pivotal role in defining the system's sensitivity, linearity, and reliability under low-photon conditions such as turbid or deep aquatic environments. Conventional SiPMs predominantly utilize surface pixel architectures, in which the photosensitive avalanche region is located directly beneath the top layer. While widely adopted due to their manufacturability and compactness, surface-pixel SiPMs are inherently limited by reduced fill factor and photon losses due to reflective metal routing and passivation layers on the surface,[8–10] (figure 2 a-Model MPPC S12572-010P). The conventional architecture is based on a surface-pixel layout composed of microcells integrated onto a common silicon substrate 1. The substrate is typically fabricated using the Czochralski or float-zone method, ensuring high crystalline purity and suitable electrical conductivity for avalanche multiplication. Each microcell, or pixel 2, has a lateral size of 10 μm, which directly influences the detector's fill factor and spatial resolution. Central to the functionality of each pixel is the quenching resistor 3, a thin-film component with resistance of 100 kΩ. This resistor ensures that the avalanche process, once triggered by a single photon event, is rapidly quenched to allow for pixel recovery and repeated detection. A common contact bus 4 distributes the bias

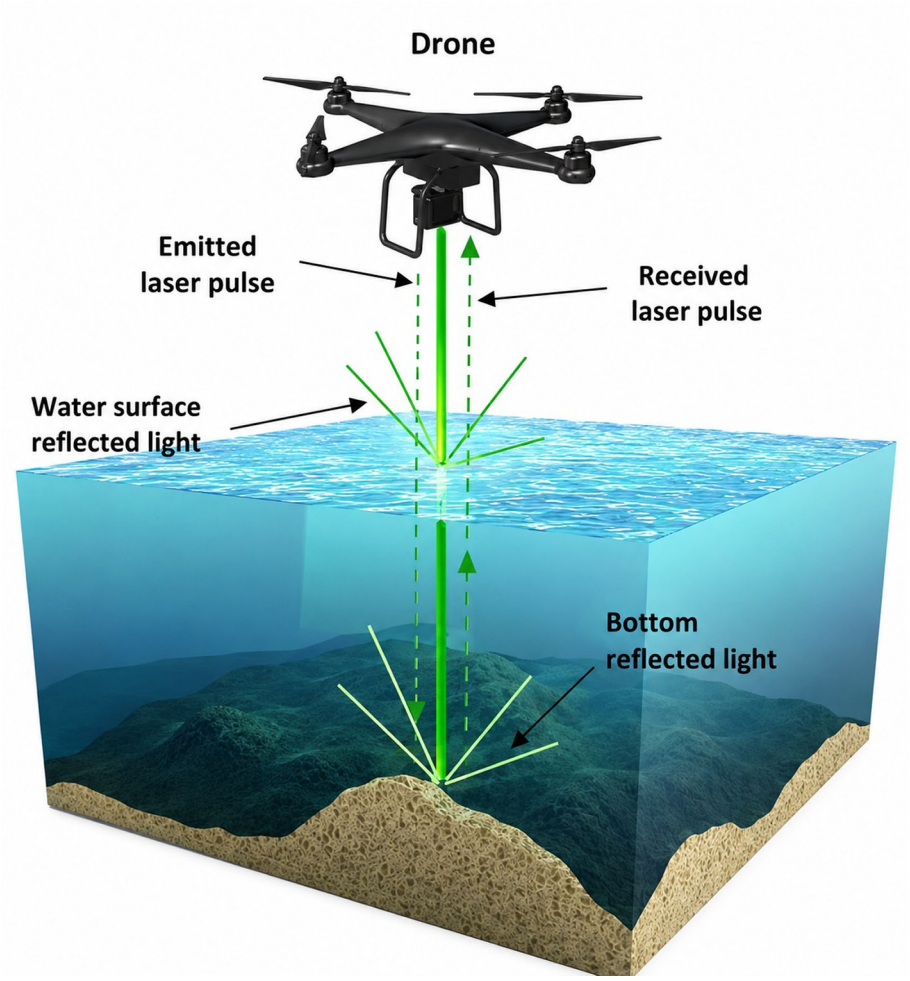


Figure 1. Schematic diagram of the bathymetric LiDAR system illustrating the time-of-flight (ToF) measurement principle.

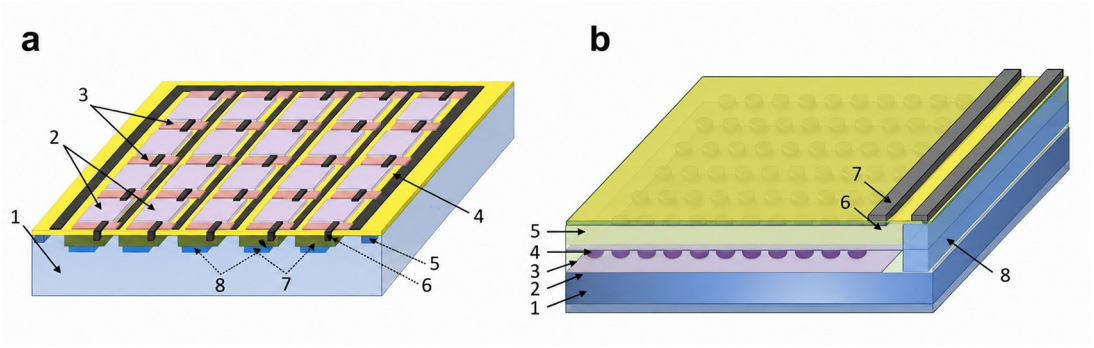


Figure 2. (a) Structure of the conventional surface-pixel SiPM (MPPC S12572-010P). (b) Structure of the buried-pixel SiPM (MAPD-3NM-II).

voltage uniformly across all pixels. Each pixel connects to the bus via its dedicated quenching resistor, supporting independent operation and minimizing dead time. To prevent unwanted edge breakdown and premature triggering near the periphery of the device, a guard ring 5 is employed. This ring suppresses high electric field concentrations at the detector's boundaries, thereby enhancing breakdown voltage uniformity and improving overall stability. The contact area 6 comprises metalized regions that provide electrical access to the external circuitry. It is carefully designed to avoid

significant obstruction of incident light. The photosensitive area 7 represents the active region of the SiPM where incoming photons are absorbed and generate electron-hole pairs; optimizing this region for minimal reflection and high transparency is essential for maximizing PDE. Finally, the avalanche area 8, located within each pixel, contains the p-n junction designed to operate in Geiger mode. When a photon-induced carrier enters this region, it initiates an avalanche multiplication event, producing a detectable signal pulse.

Figure 2. SiPM with surface pixel structure (a) and buried pixel structure (b).

In contrast, the developed buried pixel structure employs a deep-substrate architecture,[11–16] where the avalanche multiplication region is embedded beneath a transparent, passivated top layer, eliminating the need for direct metal contact in the active detection zone. This design significantly increases the effective fill factor (100%), and enhances the PDE by reducing surface optical dead zones. The deeper electric field geometry also helps to improve uniformity of gain and timing resolution across the micro-pixel array. To address the inherent limitations of surface-pixel SiPM architectures, a proposed buried pixel detector design has been developed, as shown in Figure 2b (Model MAPD-3NMII). This advanced structure begins with a high-purity silicon substrate 1, selected based on its conductivity type and grown using the Czochralski or float-zone method to ensure structural uniformity and minimal defect density. The device incorporates an n-type layer 2 as the base, which plays a critical role in defining the electric field distribution and supporting the charge collection from the multiplication region. Above this lies the first p-type epitaxial layer 3, which is essential for forming the buried junction and guiding the avalanche process away from the surface, thereby improving detection uniformity and reducing surface-related noise. The pixel 4 in this architecture is notably smaller—10 μm—allowing for higher spatial resolution and improved fill factor within a densely packed array. A second p-type epitaxial layer 5 is introduced to fine-tune the vertical electric field profile and enhance the avalanche confinement deep within the substrate. This dual-epitaxy structure not only boosts the PDE by maximizing the active volume but also improves gain uniformity across the device. The contact area 6 is designed to ensure efficient biasing without obstructing incident photons, while aluminum contacts 7 are used to establish electrical connectivity with external circuits, selected for their compatibility with CMOS integration and excellent conductivity. To mitigate edge-related electrical stress and suppress premature breakdown phenomena, a guard ring 8 is incorporated at the periphery of the detector. This structural feature ensures stable high-voltage operation and extends the breakdown threshold of the device, making it suitable for high-gain, low-noise applications in precision photon counting.

The breakdown voltage (U_{break}) is a key parameter for each SiPM and must be accurately defined (Figure 3). This was achieved by calculating the derivative of the current J with respect to voltage U, normalized by the current itself, as expressed by the following expression $\frac{dJ(U)}{dU}$. The breakdown voltage was defined as the voltage corresponding to the maximum value of the rate of change of the current.

Figure 3. Determination of breakdown voltages.

Figure 4 illustrates the dependence of the internal gain on the applied reverse voltage for the MPPC S12572-010P (left) and the MAPD 3NM-II (right) measured at room temperature (~23 °C). The internal gain M at various reverse voltages was determined using the following equation:

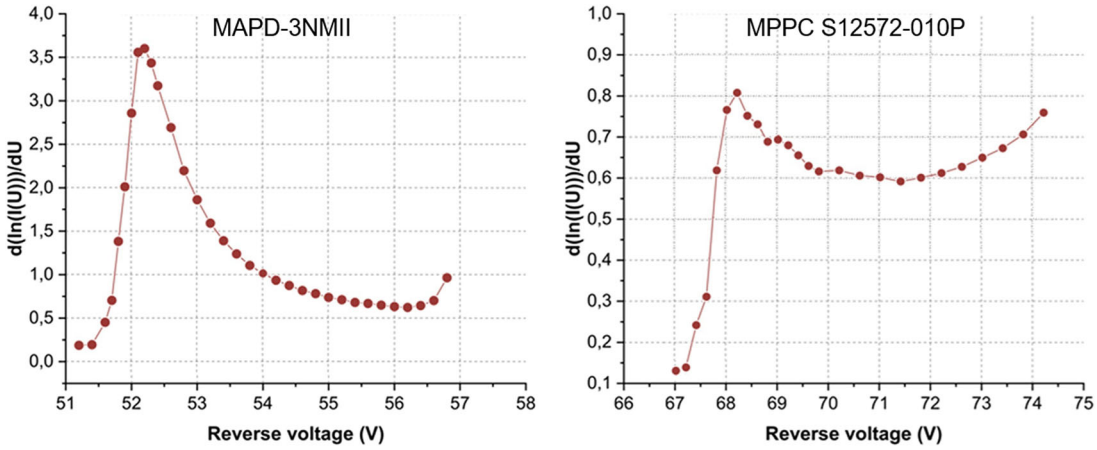


Figure 3. Determination of the breakdown voltage from the normalized current derivative.

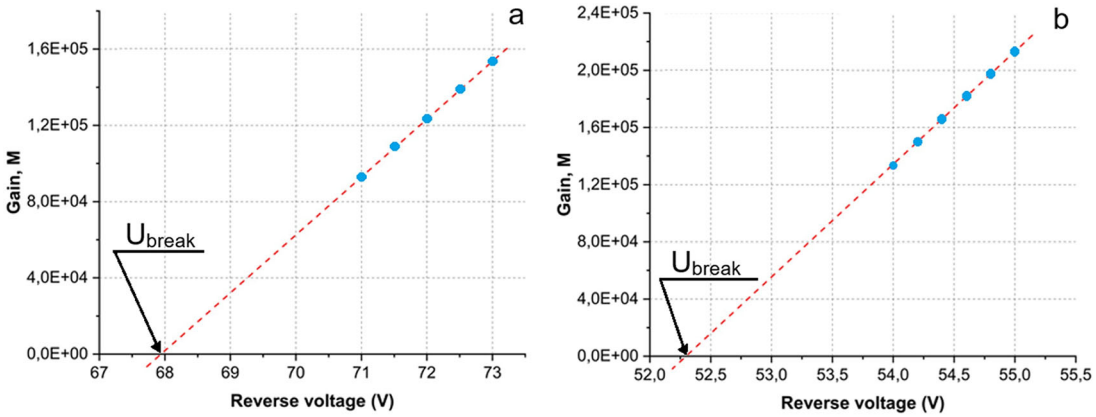


Figure 4. Dependence of the internal gain on the applied reverse voltage for the MPPC S12572-010P and MAPD-3NM-II measured at room temperature.

$$M = \frac{m * C_{pixel} * (U_{oper} - U_{break})}{q} = \frac{A_{average} * 40fC}{G_{am} * q}$$

where C_{pixel} - pixel capacitance, Uapp.v - the applied voltage ($U_{oper} \geqslant U_{break}$), U_{break} - the breakdown voltage, m - coefficient which may change from 1 to 2 depending on the values of resistance of the depletion layer and the capacitance of the pixel, G_{am} - the amplification coefficient of the amplifier or preamplifier (100 times), q - electron charge and $A_{average}$- the corresponding ADC channel number (40fC charge per chanel) to the amplitude of a single photoelectron. A linear increase in gain with increasing reverse voltage is observed. The extrapolated intersection of the linear fit with the voltage axis, corresponding to a gain approaching zero, was identified as the breakdown voltage ($U_{oper} \approx U_{break}$). The breakdown voltages obtained from the gain analysis are close in value, amounting to approximately 52.3 V for the MAPD 3NM-II and 68 V for the MPPC S12572-010P.

Figure 4. The dependence of the gain on the applied voltage for MPPC-S12572-010P (left) and MAPD 3NM-II (right) at room temperature (~23 °C).

The photon detection efficiency of the MAPD-3NM-II photodiode and the MPPC S12572-010P was evaluated using a pulsed single-photon counting technique. The measurements were performed with a pulsed green laser source operating at a wavelength of 530 nm. Accurate application of the single-photon counting approach requires sufficient pedestal statistics. At low overvoltage values (approximately 1 V), the method becomes unreliable due to broadening of the pedestal peak, whereas at high overvoltages (around 5 V), increased dark count rates and optical cross-talk significantly distort the spectra. For this reason, PDE measurements were conducted at intermediate overvoltages.

A comparative analysis of the PDE was carried out under two different conditions: identical applied overvoltage and identical internal gain. The pulse-height spectra recorded at an overvoltage of 4 V and at a gain close to 10^5 in Fig. 5. In all cases, the mean number of photons per pulse incident on the active area of both detectors was maintained at the same level. At an overvoltage of 4 V, the internal gain of the MAPD-3NM-II reached $1.2*10^5$, while the MPPC S12572-010P exhibited a gain of 8.5×10^4. Under identical overvoltage conditions, the PDE was found to be 32% for the MAPD-3NM-II and 8% for the MPPC S12572-010P. When comparing the detectors at equal gain, the PDE of the MPPC increased to 9.5%, whereas the MAPD-3NM-II maintained a value of 32%. This substantial discrepancy is mainly attributed to differences in the geometrical fill factor: approximately 33% for the S12572-010P and 100% for the MAPD-3NM-II.

Figure 5. Pulse-height distributions of the surface-pixel (MPPC S12572-010P) and buried-pixel (MAPD-3NM-II) structures at the same overvoltage of 4 V (left) and at the same internal gain (right).

Conclusion

The integration of silicon photomultipliers (SiPMs) into bathymetric LIDAR systems represents a significant advancement in underwater topographic mapping, offering enhanced sensitivity, photon detection efficiency, and spatial resolution. Traditional surface-pixel SiPMs, while effective, are constrained by lower fill factors, limited dynamic range. In contrast, the newly developed buried pixel SiPM architecture, demonstrates clear advantages in photon-counting performance, linearity, and robustness under low-light aquatic conditions.

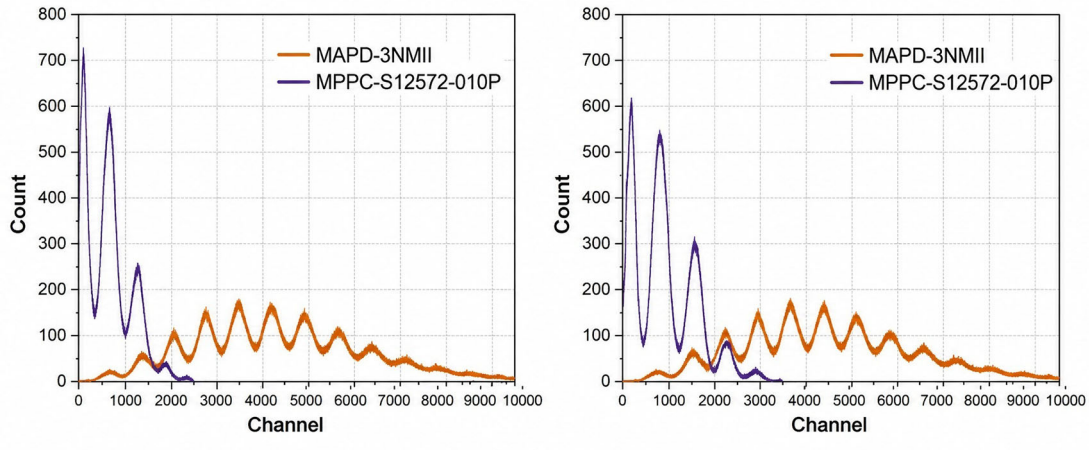


Figure 5. Pulse height distribution of surface pixel (MPPC-S12572-010P) and buried pixel (MAPD-3NMII) structures at same overvoltage of 4 V (left) and at same internal gain (right).

Spectral analyses confirm the superior photon resolution of buried pixel devices, exhibiting well-defined multi-photon peaks (up to 10 or more) in charge histograms—compared to the 5 peaks typically observed in surface-pixel designs. This enhancement is directly attributable to increased fill factor, improved avalanche confinement, and optimized field uniformity. These features make the buried structure particularly well-suited for integration into compact, drone-mounted LIDAR systems that require both mechanical durability and ultra-low photon threshold detection.

In conclusion, buried pixel SiPM technology offers a transformative solution for advancing LIDAR-based bathymetry, addressing longstanding challenges in photodetector efficiency, resolution, and environmental adaptability. Continued development and optimization of this architecture are expected to drive significant progress in photon-counting instrumentation for marine science and remote sensing.

Ethics and consent

Ethical approval and consent were not required for this study because no human participants, animals, or personal data were involved.

Data availability

The underlying data supporting the results of this study are openly available in the Zenodo repository at https://doi.org/10.5281/zenodo.22067105.[17]

This project contains the following data: figure files and the underlying numerical data in Excel format used to generate the figures and support the results presented in the manuscript.

Data are available under the terms of the Creative Commons Attribution 4.0 International license (CC-BY 4.0).

References

1. Zhou G, Liu Z, Zhou X, *et al.*: **Internal stray light suppression for single-band bathymetric LiDAR optical system.** *IEEE Trans. Instrum. Meas.* 2024; **73**: 1–12.
Publisher Full Text

2. Rumbaugh LK, Bollt EM, Jemison WD, *et al.*: **A 532 nm chaotic lidar transmitter for high resolution underwater ranging and imaging.** *In 2013 OCEANS-San Diego.* IEEE; 2013, September; 1–6.

3. Wu J, Qian Z, Zhao Y, *et al.*: **64× 64 GM-APD array-based readout integrated circuit for 3D imaging applications.** *SCIENCE CHINA Inf. Sci.* 2019; **62**(6): 62407.
Publisher Full Text

4. Ruch ML, Sivels CB, Czyz SA, *et al.*: **Comparison between silicon photomultipliers and photomultiplier tubes for pulse shape discrimination with stilbene.** *2014 IEEE Nuclear Science Symposium and Medical Imaging Conference (NSS/MIC).* IEEE; 2014, November; 1–3.

5. Ma Y, Zhang B, Chen X, *et al.*: **Theoretical detection model of SiPM-based photon-counting lidars and performance analysis under different discrimination thresholds.** *Opt. Express.* 2025; **33**(15): 32298–32319.
Publisher Full Text

6. Taneski F, Gyongy I, Al Abbas T, *et al.*: **Guided direct time-of-flight LiDAR using stereo cameras for enhanced laser power efficiency.** *Sensors.* 2023; **23**(21): 8943.
PubMed Abstract | Publisher Full Text | Free Full Text

7. Holzhüter H, Bödewadt J, Bayesteh S, *et al.*: **Technical concepts of automotive LiDAR sensors: a review.** *Opt. Eng.* 2023; **62**(3):

031213–031213.
Publisher Full Text

8. Zhang C, Zhang G, Cao X, *et al.*: **Methodology for measuring the fill factor of silicon photomultipliers.** *Measurement.* 2023; **213**: 112720.
Publisher Full Text

9. Fischer P, Keller M, Ritzert M: **Design of a large area digital SiPM with high fill factor and fully serial digital readout for single photon detection in liquid noble gas detectors.** *J. Instrum.* 2025; **20**(06): C06008.
Publisher Full Text

10. Del Guerra A, Belcari N, Bisogni MG, *et al.*: **Advantages and pitfalls of the silicon photomultiplier (SiPM) as photodetector for the next generation of PET scanners.** *Nucl. Instrum. Methods Phys. Res., Sect. A.* 2010; **617**(1–3): 223–226.
Publisher Full Text

11. Sadygov Z, Olshevski A, Chirikov I, *et al.*: **Three advanced designs of micro-pixel avalanche photodiodes: Their present status, maximum possibilities and limitations.** *Nucl. Instrum. Methods Phys. Res., Sect. A.* 2006; **567**(1): 70–73.
Publisher Full Text

12. Nuruyev S, Ahmadov G, Sadigov A, *et al.*: **Performance of silicon photomultipliers at low temperature.** *J. Instrum.* 2020; **15**(03): C03003.
Publisher Full Text

13. Ahmadov F, Ahmadov G, Mammadli A, *et al.*: **Study of the neutron radiation hardness of MAPD-3NK2 silicon photomultipliers.** *Sci. Rep.* 2025; **15**(1): 40974.
Publisher Full Text

14. Nuriyev S, Ahmadov F, Sadygov Z, *et al.*: **Performance of a new generation of micropixel avalanche photodiodes with high pixel density and high photon detection efficiency.** *Nucl. Instrum. Methods Phys. Res., Sect. A.* 2018; **912**: 320–322.
Publisher Full Text

15. Ahmadov F, Abdullayev F, Ahmadov G, *et al.*: **A new physical model of Geiger-mode avalanche photodiodes.** *J. Instrum.* 2020; **15**(01): C01009.
Publisher Full Text

16. Ahmadov F, Ahmadov G, Sadygov A, *et al.*: **Performance of LaBr3 (Ce) scintillator with MAPD readout in the gamma-ray energy range of 0.1–7.0 MeV.** *Radiation Detection Technology and Methods.* 2025; **9**: 563–569.
Publisher Full Text

17. Huseynzada K, Sadigov A, Lyubchyk S: **Silicon photomultipliers for enhanced lidar bathymetric applications.** *Zenodo* 2026, July 21.
Publisher Full Text